Hindawi
Advances in Materials Science and Engineering
Volume 2020, Article ID 5453703, 11 pages
https://doi.org/10.1155/2020/5453703

Research Article

Study on Friction and Wear Behavior of Inconel 625 Superalloy during Hot Extrusion

Yanjiang Wang,[1] Sixiang Zhao,[2] Zhi Jia,[1,2] Jinjin Ji,[3] Dexue Liu,[2] Tingbiao Guo,[2] and Yutian Ding[2]

[1]*School of Materials Science and Engineering, Lanzhou University of Technology, Lanzhou 730050, China*
[2]*State Key Laboratory of Advanced Processing and Recycling of Nonferrous Metals, Lanzhou University of Technology, Lanzhou 730050, China*
[3]*School of Materials Engineering, Lanzhou Institute of Technology, Lanzhou 730050, China*

Correspondence should be addressed to Zhi Jia; jiazhi@lut.edu.cn

Received 17 September 2019; Revised 4 January 2020; Accepted 24 January 2020; Published 27 February 2020

Academic Editor: Georgios Maliaris

Friction during the hot extrusion of Inconel 625 superalloy tubes causes severe wear of the mold and plays a decisive role in the quality of the workpieces. In this paper, a ball-to-disk method was utilized to investigate the tribological behavior of Inconel 625 using two different tribological pairs, i.e., GCr15 and Si_3N_4, at room and elevated temperatures. Friction coefficient, specific wear rate, and morphology of worn surfaces were systematically characterized. It was found that the friction coefficients for both tribological pairs generally increased as the testing temperature increased, while the specific wear rate increased firstly and then decreased with the rise of temperature. Along with the increasing sliding speed, the friction coefficient between Inconel 625 and Si_3N_4 decreased monotonically, while the specific wear rate increased firstly and then decreased. Under any given testing condition, the friction coefficient and specific wear rate of the Inconel 625 for Inconel/Si_3N_4 pair are less than those of the Inconel/GCr15 pair. The main wear mechanisms between GCr15 and Inconel 625 are adhesive and fatigue wear at all testing temperatures. The wear mechanisms between Si_3N_4 and Inconel 625 are adhesive and abrasive wear at room temperature but fatigue wear at 500°C. Our findings indicate that the use of ceramic molds in the hot extrusion of Inconel 625 may significantly improve the surface qualities of the product and reduce the wear of the mold.

1. Introduction

Inconel 625 superalloy is a solid solution-strengthened nickel-based wrought superalloy with Mo and Nb as the main strengthening elements. Inconel 625 superalloy has been used in aerospace, chemical, nuclear, and other fields operating at high temperatures due to its excellent corrosion resistance, thermal stability, fatigue resistance, and oxidation resistance [1–4]. Currently, Inconel 625 superalloy tubes are mainly formed by hot extrusion. Due to the complex high-temperature and high-pressure process of hot extrusion, problems of friction, wear, and lubrication exist during hot extrusion process [5–10]. The friction between the side surface of the ingot and the wall of the extrusion cylinder during extrusion is one of the most important factors affecting the flow of the metal [11–13]. During normal extrusion, the Inconel 625 superalloy slides against the mold, and the friction force consists of the tearing force, furrowing force, and molecular adsorption force at the adhesion point of the asperities [14–20]. The friction during extrusion not only has a great influence on the performance and surface quality of the workpieces but also accelerates the wear of the mold and shortens the service life of the mold [21]. Currently, most research studies on mechanical friction and fretting friction are insufficient to describe the friction between materials and molds during extrusion. Jayaseelan et al. [22] determined the friction coefficients under nonlubricated and lubricated conditions by comparing the experimental value and simulation value of AA6063 extrusion with hot die steel (H13). Huang et al. [23] investigated the friction coefficients and

wear rates of different superalloys (GH605, GH2123, and GH4169) and Si_3N_4 pairs at different temperatures. At room temperature, the wear mechanism of GH605 and GH2132 alloys is adhesive wear, while the wear mechanism of GH4169 alloy is abrasive wear. As the temperature increases to 800°C, oxidative wear plays a significant role in the wear mechanism of Si_3N_4. Zhu et al. [24] reviewed the research progress of tool wear during nickel-based superalloy processing and analyzed the influence of various processing parameters on the wear mechanisms. Birol [25] compared the high-temperature wear behavior of Inconel 617 and Stellite6 alloys with X32CrMoV33 thermal tool steel, indicating that the former shows better wear resistance.

In this paper, the tribological properties of Inconel 625 superalloy during hot extrusion are investigated, and the friction coefficient and specific wear rate at different temperatures, different friction rates, and for different mold materials are simulated using ball-disk experiments. Through the observations and analyses of the surface wear phenomenon of Inconel 625 superalloy, the wear mechanisms were discussed and, the contributing factors were determined. These results will provide guidance for understanding the wear mechanisms of Inconel 625 superalloy and the mold during extrusion, improving the microstructures and surface qualities of the workpieces, and extending the life of the mold.

2. Experimental Procedure

An Inconel 625 ingot was extruded with a 55 MN horizontal extruder, which uses GCr15 as the mold material, at Jinchuan company, China. After extrusion, the surface of the wrought ingot is shown in Figure 1. Scratches, cracks, and delaminations are visible, indicating significant material loss.

Commercially available Inconel 625 disks and balls (6 mm in diameter) of Si_3N_4 and GCr15 were used in the ball-disk friction testing. In order to avoid any possible influence of impurities on the surface of the samples, the Inconel 625 specimens were polished up to a roughness better than 0.06 μm. Then, they were ultrasonically cleaned in acetone for 10 min and dried in hot air.

The ball-disc dry sliding wear testing was carried out using a HT-1000 high-temperature wear tester, whose working principle is schematically shown in Figure 2. The load and friction radius were set as 15 N and 5 mm, respectively. There different temperatures, i.e., 25°C, 250°C, and 500°C (with a constant heating rate of 10°C/min), and three different rotating frequencies of the friction motor, i.e., 6 Hz, 12 Hz, and 18 Hz (the corresponding sliding speeds are 175 mm/s, 350 mm/s, and 525 mm/s, respectively) were attempted. In order to ensure the same wear distance for different friction rates, the friction times were set as 45 min, 22.5 min, and 15 min, respectively.

The volumetric wear amounts were tested in a MT-500 probe-type wear scar gauge. The measuring width was 5 mm. To minimize the error, the wear amounts were measured every 120 degree on the wear mark, and the average value of the three measured results was obtained. The specific wear rate (Wer) [26] can be expressed as:

Figure 1: Surface morphology of Inconel 625 superalloy after extrusion.

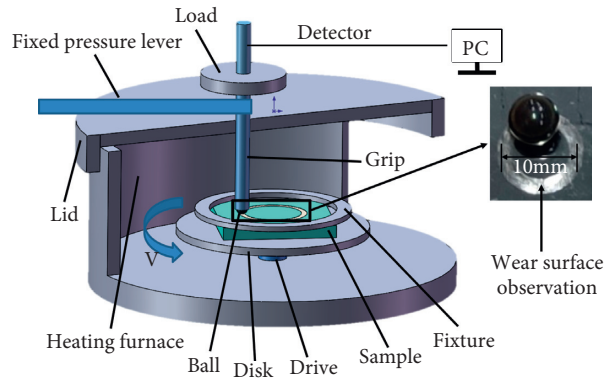

Figure 2: A sketch showing the experimental approach.

$$\text{Wer} = \frac{W}{F \cdot S}, \tag{1}$$

where W is the volume of the wear amount (mm^3), F is the friction load (N), and S is the length of the friction path (m). It should be mentioned here that ridges caused by plastic deformation were not taken into account in the calculation of W. The surfaces of the worn samples were characterized by scanning electron microscopy (SEM), and energy dispersive spectrometer (EDS). The wear marks were further observed by a Zeiss laser confocal microscope (LSM).

3. Results and Discussion

3.1. Friction Coefficients. The friction coefficients of GCr15 and Si_3N_4 balls against Inconel 625 superalloy at 525 mm/s and 250°C are shown in Figure 3. The stabilized friction coefficients of Inconel 625 superalloy on Si_3N_4 ceramic and GCr15 are about 0.17 and 0.48, respectively. By comparing the curves, it is seen that the fluctuation of friction coefficient between Inconel 625 and Si_3N_4 is less severe than that between Inconel 625 and GCr15. The comparison of optical images between Figures 3(a) and 3(b) indicates that the scars of Inconel 625 worn by GCr15 are rougher. There are many black pits on the abrasion marks, as shown in Figure 3(a), and the transition areas between the abrasion marks and intact surface are irregular.

Figure 4 shows the stabilized friction coefficients of GCr15 and Si_3N_4 against the Inconel 625 superalloy at different temperatures. With the increasing temperature, the trends of the friction coefficient for the two pairs are

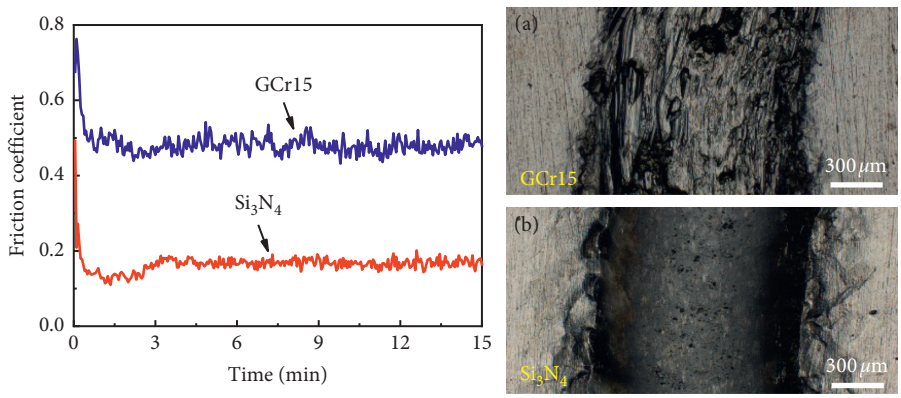

FIGURE 3: Evolution of friction coefficients between Inconel 625 disk and Si_3N_4 or GCr15 balls at a temperature of 250°C and a sliding rate of 525 mm/s. The macroscopic morphology of the wear mark by (a) GCr15 grinding and (b) Si_3N_4 grinding.

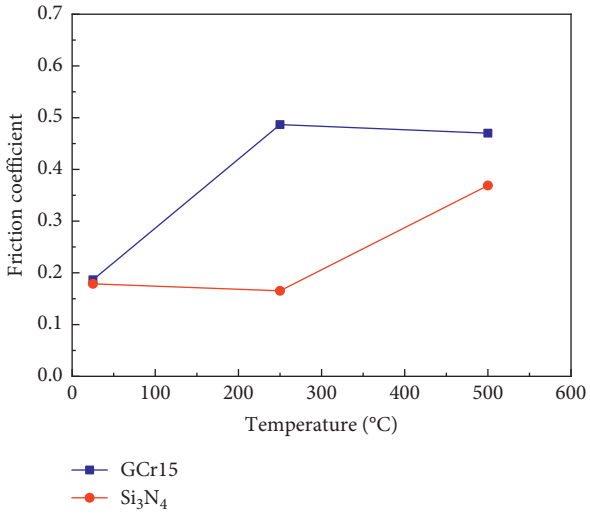

FIGURE 4: Effect of temperature on the friction coefficients of two different friction pairs at a sliding speed 525 mm/s.

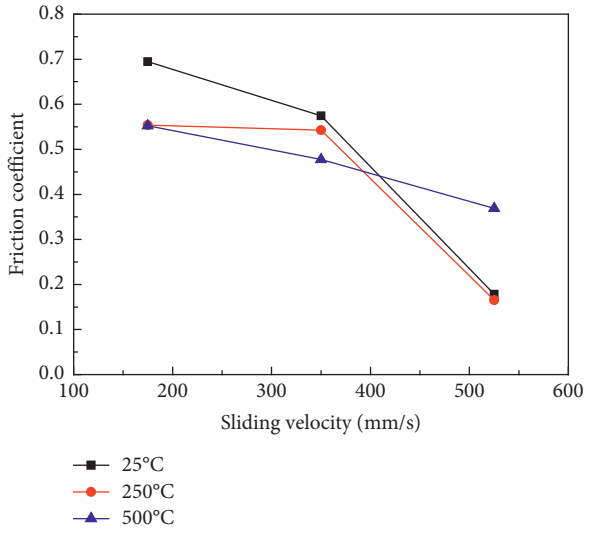

FIGURE 5: Effects of sliding speeds on the friction coefficient of Si_3N_4 against Inconel 625 under a load of 15 N at different temperatures.

different. The friction coefficient between GCr15 and Inconel 625 increases significantly with increasing temperature, and reaches a maximum value at 250°C, and then decreases slowly. Since Inconel 625 superalloy and GCr15 are both metallic materials, and have similar chemical bond, they show very high adhesive work, which makes them prone to sticking, resulting in large fluctuations of the friction coefficients. The situations for metal-ceramic pairs, however, are different. Murakami et al. [27] also found the same phenomenon the for aluminum alloy.

When Si_3N_4 is used to grind Inconel 625 superalloy, the effect of sliding speeds (175 mm/s, 350 mm/s, and 525 mm/s) on the friction coefficient is shown in Figure 5. For three different testing temperatures, the curves exhibit similar trends. The results show that at any temperature, the friction coefficient decreases with increasing sliding speed. These experimental results are consistent with a previous research [28]. For a general elastoplastic contact friction pair, with the increasing sliding speed, the friction force firstly increases to a maximum value and then decreases. Huang et al. [23] studied the change of the frictional force of Si_3N_4 on superalloys with the sliding speed. When the sliding speed is relatively low, the frictional force increases as the sliding speed increases. When the sliding speed is relatively high, the frictional force decreases as the sliding speed increases. Accordingly, there should be a sliding speed which corresponds to the peak value of the frictional force. As mentioned by many scholars [23, 29], the influence of sliding velocity on friction coefficient is closely related to the surface temperature. Sliding friction causes heating and increases the local surface temperature, thus changing the properties and failure conditions of the interacting surfaces. When the speed reaches a certain value, the surface will be heated to a flash temperature (T_f), at which the surface will be significantly softened. In this case, the shear stress will decrease, and the friction coefficient will be significantly reduced. However, when the sliding speed is 525 mm/s, the coefficient of friction of Si_3N_4 against Inconel 625 at 500°C is greater than those at 25°C and 250°C. This may be because the temperature is too high to generate oxides at the surface and much of the material is deposited on the worn surface to

form a new friction layer. Previous literature studies [23, 30] have highlighted the effect of the thickness of the friction layer on the friction coefficient.

3.2. Specific Wear Rate. Figure 6 shows the specific wear rates of the two friction pairs at different temperatures. The results show that the specific wear rate of Inconel 625 worn by Si_3N_4 is lower than that by GCr15 at all temperatures, and the trends for the two friction pairs are similar. With the increasing temperature, the specific wear rate of Inconel 625 against two kinds of friction balls firstly increases and then decreases. At 250°C, a maximum specific wear rate is observed. This is because the material softens and can be peeled easily, leading to fast wear. However, when the temperature exceeds 250°C, the specific wear rate decreases, which may be caused by the oxidation of the material surface, and the oxidation film plays a role in lubrication.

In order to deeply understand the differences in specific wear rate between the two friction pairs, the depth and width of the wear scar after wear were observed, as shown in Figure 7. It is found that materials are extruded on both sides of the wear marks generated by the GCr15 and Si_3N_4 balls, and the depths of the wear marks are roughly the same. However, the widths of the wear marks after GCr15 ball friction are relatively wider, and the two-dimensional profiles of the wear marks after GCr15 ball friction are uneven, with very narrow grooves at the bottom. On the contrary, the wear marks worn by Si_3N_4 are relatively smooth and show a U shape. This is also supported by microscopic observation of the worn surfaces of Inconel 625, as shown in Figure 8. There are large steps on the surface of the wear mark in Figure 8(a) but very slight exfoliations in Figure 8(b). This might be the reason why the friction coefficient between Inconel 625 and GCr15 is higher than between Inconel 625 and Si_3N_4. Generally, the specific wear rate has a direct relationship with the hardness of the ball, and harder balls usually generate more significant wear [31]. However, in this study, the specific wear rate of Inconel 625 by Si_3N is smaller, which can support the development of a ceramic mold.

The sliding speed has a significant influence on the specific wear rate of Inconel 625 superalloy, as shown in Figure 9. In general, at any temperature except 250°C, the specific wear rate firstly increases and then decreases with the increasing sliding speed. At a sliding speed of 350 mm/s, the specific wear rate of Inconel 625 by Si_3N_4 at 250°C reaches a lowest value, indicating this may be a critical speed. Three-dimensional contour of the worn surfaces were observed, as shown in Figure 10. When the temperature is 500°C and the sliding speed is 525 mm/s, the surface has large plastic deformation, as two large ridges are observed on the sides of the wear scar. There are many scratches on the surfaces of the wear scars. This is because the surface temperature at the contacting points rises sharply at high sliding speeds, and the material softens or even partially melts. When the sliding speed is 350 mm/s, the ridges along with the wear mark are negligible, and the surfaces at the bottom of the wear marks are seriously scratched. This result is consistent with Figure 6. When the sliding speeding is

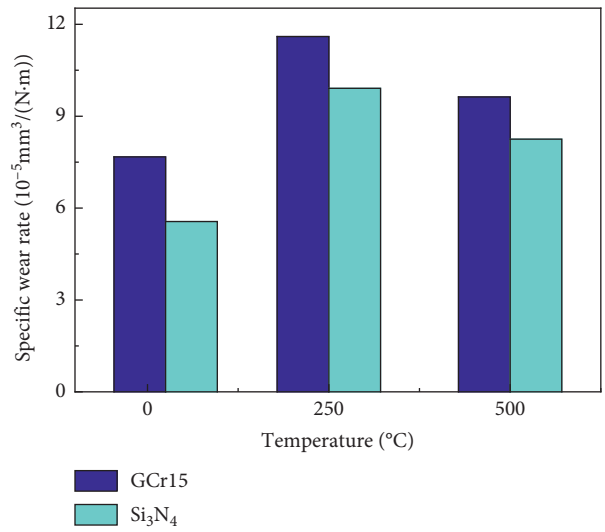

Figure 6: Effects of testing temperature on the specific wear rate of Inconel 625 superalloy at a sliding rate of 525 mm/s.

175 mm/s, the depth of the wear marks become shallow, and the wear marks are relatively smooth.

3.3. Wear Mechanism. SEM images of Inconel 625 after grinding with GCr15 balls are shown in Figure 11. In Figure 11(a), there are many layers, and the shedding fragments are relatively large. This is because adhesive wear takes place between GCr15 and Inconel 625 under the combination of compressive and shear stress, and the adhesive stress is higher than the shear strength of the base metal, thus making the surface of Inconel 625 torn. There are two different morphologies in Figure 11(c), and numerous pits are observed in the enlarged image (Figure 11(d)). As a result of the high temperature, the material is easily to deform and flake off. The small debris contacts the bottom of the wear scar repetitively under the load, thus producing fatigue and causing pits with different depths and sizes. Combined with the previous analyses, it can be found that there are two different wear mechanisms at different temperatures, i.e., the adhesive wear mechanism when the temperature is low and the adhesive wear and fatigue wear mechanisms when the temperature is high.

Figure 12 shows the SEM images of worn surfaces Inconel 625 by Si_3N_4 grinding. For the 250°C specimen, delamination is seen (Figure 12(a)). Shear damage occurs in the subsurface of the metal, causing strain on the surface material. The damages are attributable to the adhesive wear and abrasive wear. At a high temperature of 500°C, the worn surface shows peeling and steps (Figure 12(c)). The magnified image (Figure 12(d)) shows cracks on the worn surface. The cracks may be caused by fatigue at high temperatures: the cracks initiate at physical and chemical defects and then propagate under cyclic sliding.

Figure 13 shows the SEM images of Inconel 625 worn by Si_3N_4 at different sliding speeds at 500°C. The surface after 175 mm/s grinding shows patches (Figure 13(a)), and a large amount of abrasive particles and deep holes were found in the

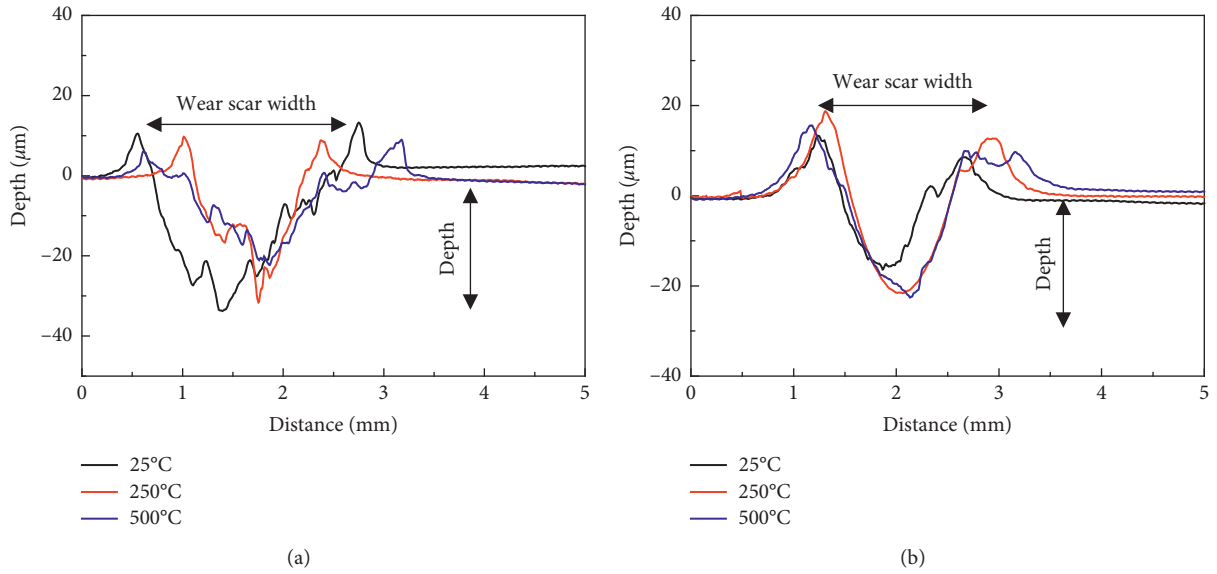

Figure 7: Two-dimensional contour of the wear scar of Inconel 625 superalloy by (a) GCr15 and (b) Si_3N_4, at a sliding speed of 525 mm/s and a load of 15 N.

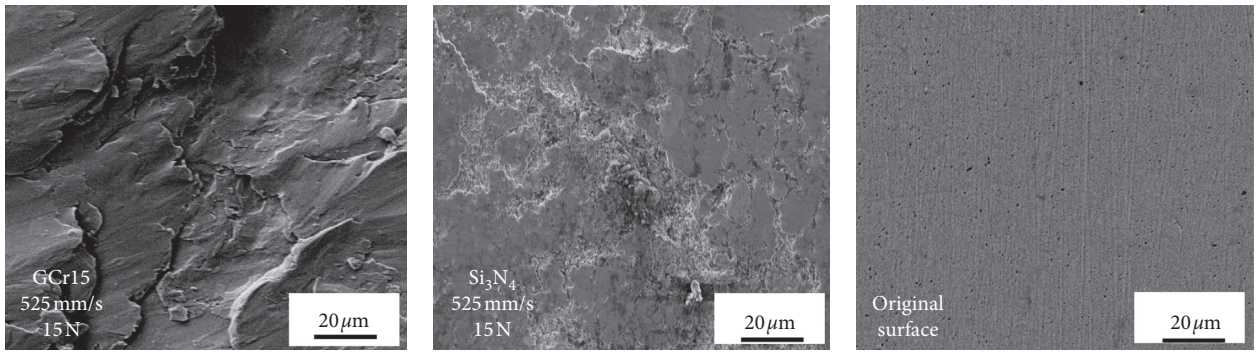

Figure 8: (a, b) SEM images of wear marks of Inconel 625 after friction at room temperature and sliding rate of 525 mm/s; (c) typical surface morphology of the original specimens.

magnified image (Figure 13(b)). In the 350 mm/s sample, several peel offs are observed on the flat wear surface, as shown in Figure 13(d). It is supposed that the abrasive debris was not taken away from the sliding track timely when the sliding speed is low, thus resulting in abrasive wear. The deep holes may be caused by the internal structural changes and defects of the material induced by high temperatures. In the 350 mm/s specimen, the bulges in the wear scar may be caused by the oxidation of the material, thus leading to an oxidative wear.

The SEM images of the surfaces of Inconel 625 worn at different sliding speeds at room temperature are shown in Figure 14. It can be seen that, at a speed of 175 mm/s, the surface of the material creates furrows along the sliding direction (Figures 14(a) and 14(b)). At a speed of 350 mm/s, there are many hollows on the worn surface (Figure 14(c)). In the magnified image (Figure 14(d)), it is found that there are many pits in the hollows (Figure 14(d)). It has been found that at room temperature, when the speed is 175 mm/s, the material on the surface of the metal is ploughed to form a groove. This is because the strength of the abrasive grains formed at a low sliding speed at a low temperature is high, and the furrow wear is formed. When the speed is 350 mm/s, the surfaces may be subjected to complex stress forms and even stress concentration, resulting in damages such as peeling off and fatigue wear.

By comparing the SEM images of the wear surface of Inconel 625 superalloy with GCr15 and Si_3N_4 balls, it is found that the wear behavior of the Inconel 625 under all studied conditions is different, and the mechanisms of the wear are rather complex. When GCr15 is used to grind Inconel 625 superalloy, the wear mechanism is induced by adhesive wear. When Si_3N_4 is used to grind Inconel 625 superalloy, the subsurface of the material is prone to damage, resulting in wear. EDS analyses and cross-section corrosion studies were performed on the worn surface, as shown in Figures 15 and 16. In spectrum 2, the distribution of main

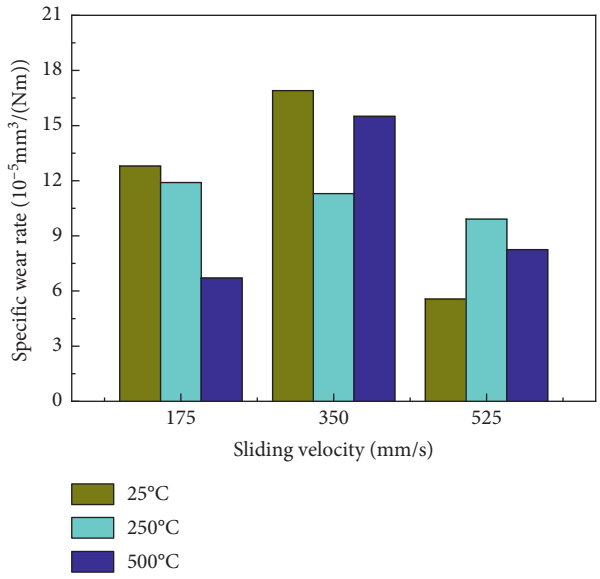

Figure 9: Effect of sliding speed on the specific wear rate of Inconel 625 by Si_3N_4 at different temperatures, under a load of 15 N.

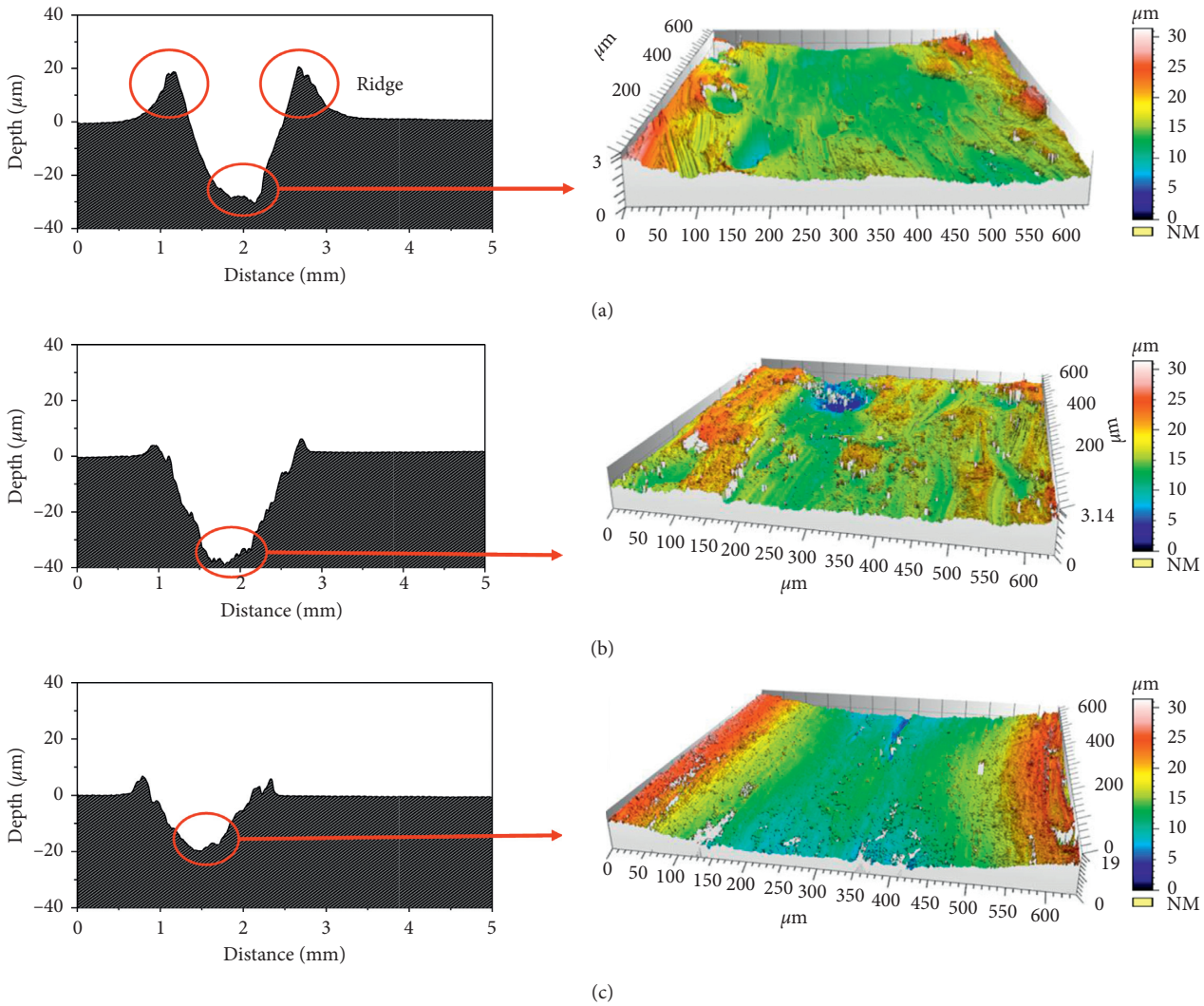

Figure 10: Three-dimensional morphologies of the wear surfaces of Inconel 625 by Si_3N_4 at different sliding speeds at a temperature of 500°C and under a load of 15 N (a) 525 mm/s, (b) 350 mm/s, and (c) 175 mm/s.

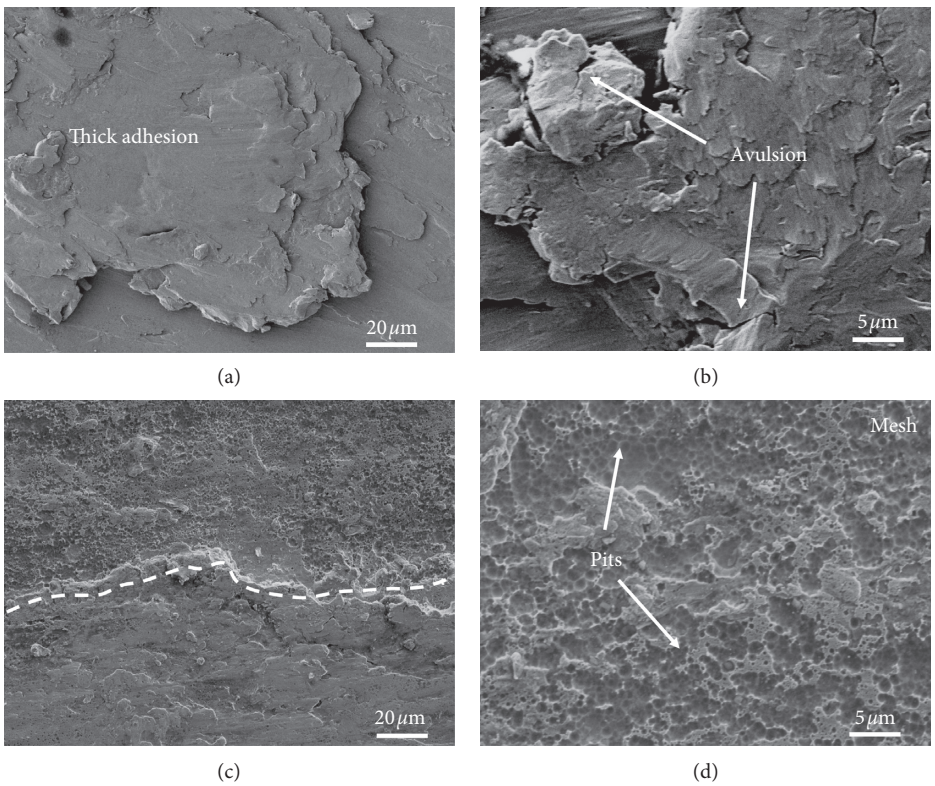

Figure 11: SEM images of the surfaces of Inconel 625 worn by GCr15: (a) 25°C, 525 mm/s, 15 N; (c) 500°C, 525 mm/s, 15 N; (b, d) enlarged views of (a) and (c), respectively.

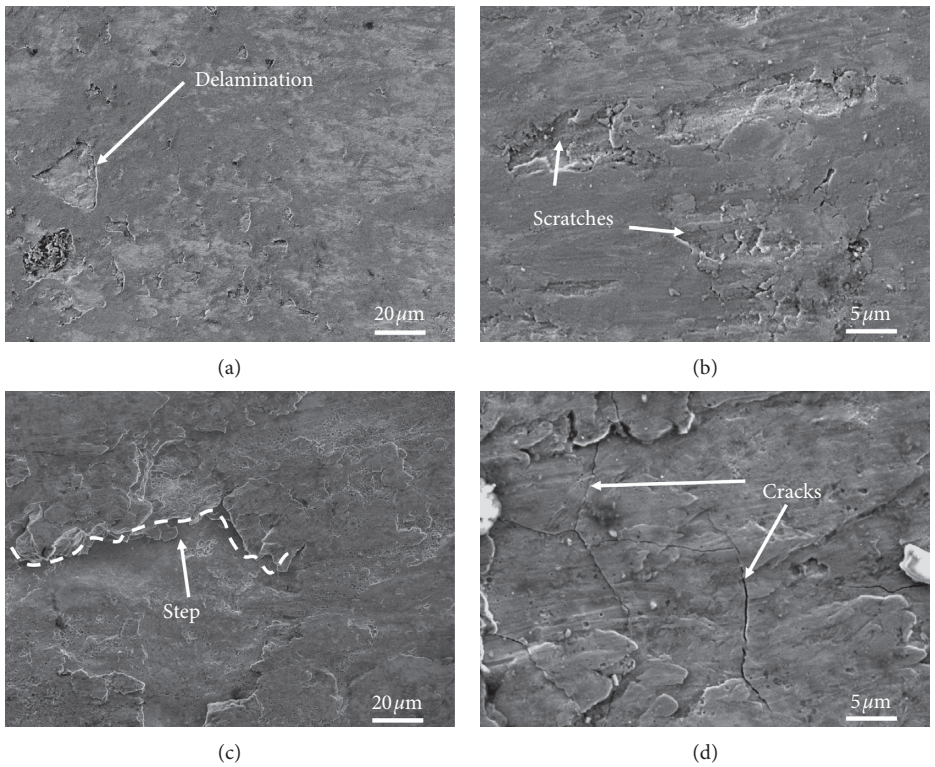

Figure 12: SEM images of the surfaces of Inconel 625 worn by Si_3N_4: (a) 250°C, 525 mm/s, 15 N; (c) 500°C, 525 mm/s, 15 N; (b, d) enlarged images corresponding to (a) and (c), respectively.

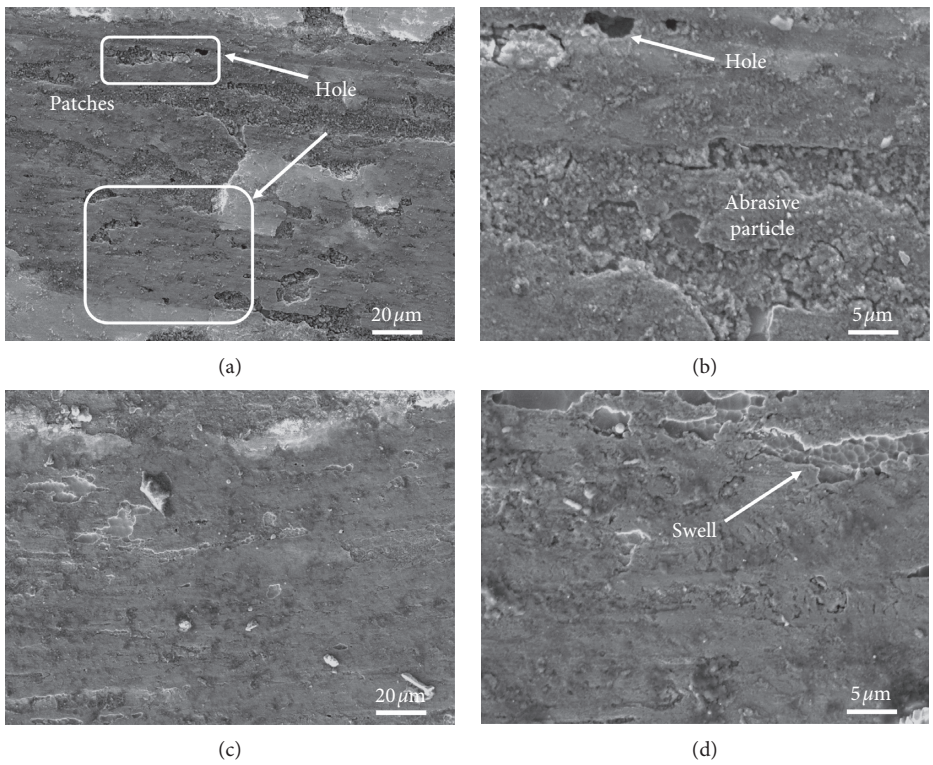

Figure 13: SEM images of the worn surfaces of Inconel 625 after grinding with Si_3N_4 at 500°C: (a) 175 mm/s, 15 N; (c) 350 mm/s, 15N; (b, d) enlarged views of (a) and (c), respectively.

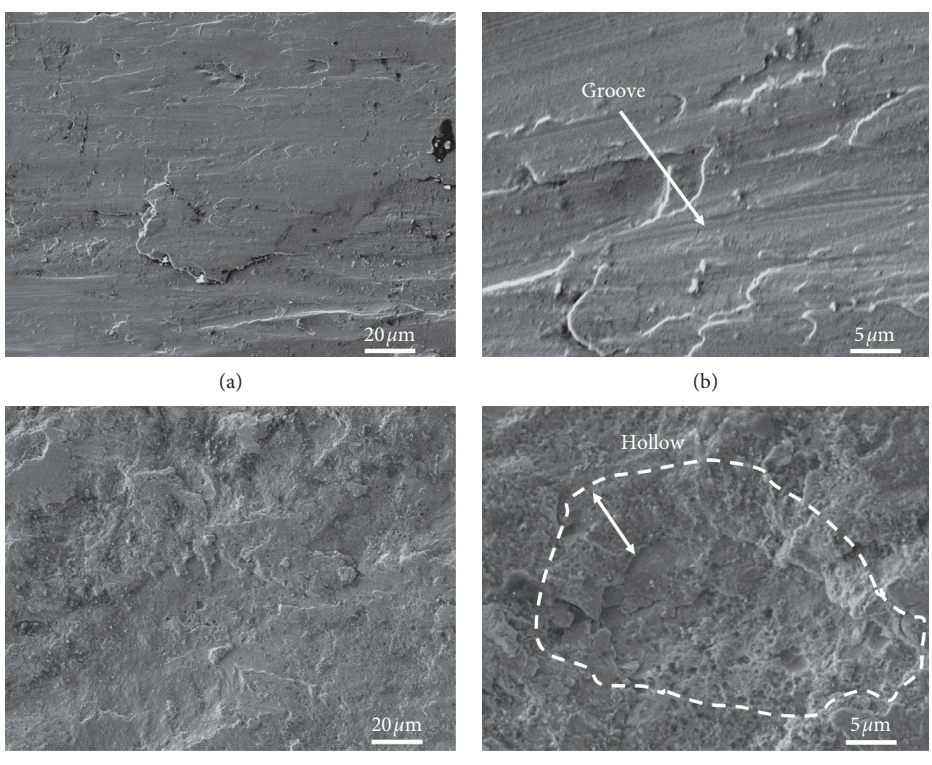

Figure 14: SEM images of the wear surfaces of Inconel 625 superalloy after Si_3N_4 grinding at 25°C: (a) 175 mm/s, 15 N; (c) 350 mm/s, 15 N; (b, d) enlarged views of (a) and (c).

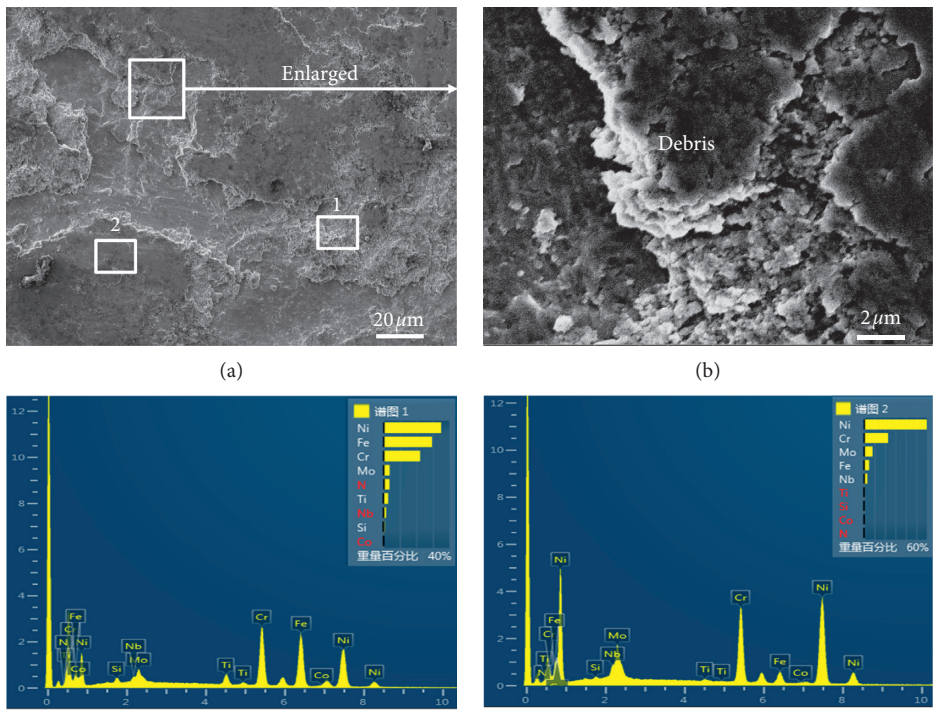

Figure 15: SEM images of the wear surfaces of Inconel 625 superalloy after Si_3N_4 grinding: (a) 25°C, 525 mm/s, 15 N; (b) enlarged view of (a); (c, d) EDS of the 1 and 2 regions.

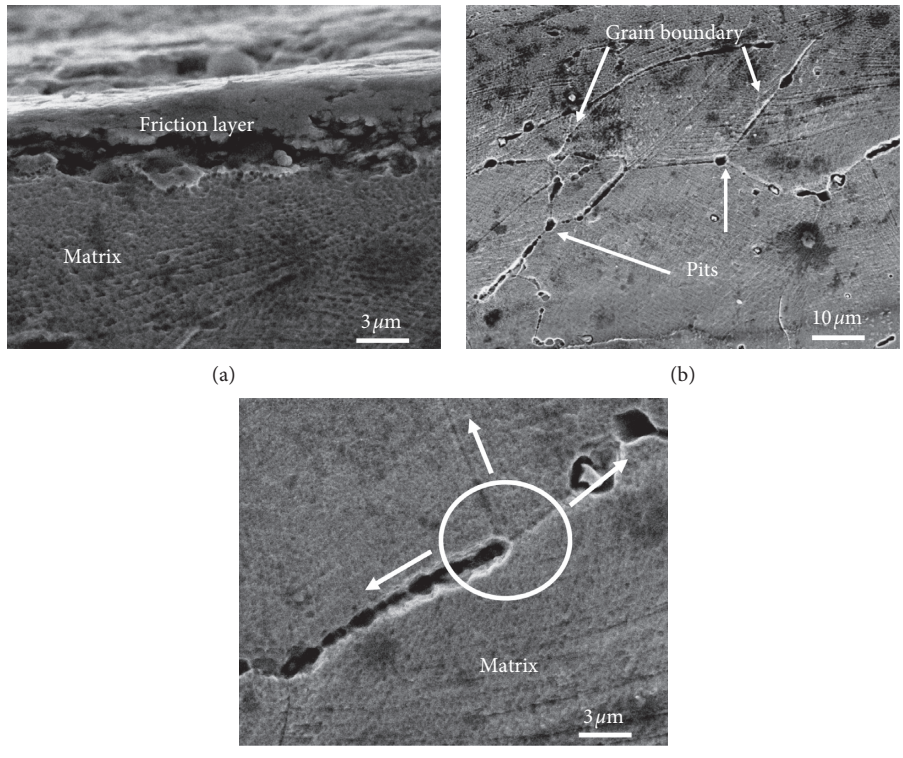

Figure 16: Cross-sectional SEM images of the worn Inconel 625 superalloy: (a) 25°C, 525 mm/s, 15 N; (b) SEM images after cross-section corrosion; (c) enlarged view of (b) after corrosion of the cross section.

elements is similar to that of Inconel 625. However, in spectrum 1, the contents of Fe and Cr are higher than those in Inconel 625. Both the elements react with oxygen in the surrounding environment during wear. It can be seen from the cross-sectional SEM images that the wear surface friction layer and the substrate are separated by obvious boundary lines (Figure 16(a)). When the cross-section was polished and corroded, it is found that the grain boundaries are less corrosion-resistant (Figures 16(b) and 16(c)), which may be caused by damages caused by grinding. These results may lead to accelerated wear and new wear mechanisms.

4. Conclusions

(1) When Si_3N_4 and GCr15 balls slide against Inconel 625 superalloy, the friction coefficient increases with an increase in temperature and decreases with the increase in sliding speed. Moreover, the friction coefficient and specific wear rate of the Si_3N_4 ball in grinding the Inconel 625 superalloy are less than that of the GCr15 ball.

(2) The wear mechanisms of Inconel 625 superalloy are primarily adhesive wear and abrasive wear when the temperature and speed are low, and fatigue plays a key role at high temperature and high speed.

(3) Our study indicates that the use of ceramic molds for hot extrusion of Inconel 625 can significantly improve the surface quality of the product and reduce the wear of the mold.

Data Availability

The data used to support the findings of this study are included within the article.

Conflicts of Interest

The authors declare that they have no conflicts of interest.

Acknowledgments

This project was supported by the National Nature Science Foundation of China (nos. 51665032 and 51664041), Science Foundation for Distinguished Young Scholars of Gansu Province (18JR3RA134).

References

[1] J. McCarley, B. Alabbad, and S. Tin, "Influence of the starting microstructure on the hot deformation behavior of a low stacking fault energy Ni-based superalloy," *Metallurgical and Materials Transactions A*, vol. 49, no. 5, pp. 1615–1630, 2018.

[2] R. T. Foley, M. B. Peterson, and C. Zapf, "Frictional characteristics of cobalt, nickel, and iron as influenced by their surface oxide films," *A S L E Transactions*, vol. 6, no. 1, pp. 29–39, 1963.

[3] X. Yang, W. Li, J. Li et al., "Finite element modeling of the linear friction welding of GH4169 superalloy," *Materials & Design*, vol. 87, pp. 215–230, 2015.

[4] S. Hanasaki, J. Fujiwara, M. Touge, Y. Hasegawa, and K. Uehara, "Tool wear of coated tools when machining a high nickel alloy," *CIRP Annals*, vol. 39, no. 1, pp. 77–80, 1990.

[5] A. T. Alpas, H. Hu, and J. Zhang, "Plastic deformation and damage accumulation below the worn surfaces," *Wear*, vol. 162–164, pp. 188–195, 1993.

[6] W. M. Rainforth, R. Stevens, and J. Nutting, "Deformation structures induced by sliding contact," *Philosophical Magazine A*, vol. 66, no. 4, pp. 621–641, 1992.

[7] A. Moshkovich, V. Perfilyev, T. Bendikov, I. Lapsker, H. Cohen, and L. Rapoport, "Structural evolution in copper layers during sliding under different lubricant conditions," *Acta Materialia*, vol. 58, no. 14, pp. 4685–4692, 2010.

[8] A. Moshkovich, I. Lapsker, Y. Feldman, and L. Rapoport, "Severe plastic deformation of four FCC metals during friction under lubricated conditions," *Wear*, vol. 386–387, pp. 49–57, 2017.

[9] L. Wang, R. W. Snidle, and L. Gu, "Rolling contact silicon nitride bearing technology: a review of recent research," *Wear*, vol. 246, no. 1–2, pp. 159–173, 2000.

[10] L. X. Li, D. S. Peng, J. A. Liu, Z. Q. Liu, and Y. Jiang, "An experimental study of the lubrication behavior of A5 glass lubricant by means of the ring compression test," *Journal of Materials Processing Technology*, vol. 102, no. 1–3, pp. 138–142, 2000.

[11] M. Bakhshi-Jooybari, "A theoretical and experimental study of friction in metal forming by the use of the forward extrusion process," *Journal of Materials Processing Technology*, vol. 125–126, pp. 369–374, 2002.

[12] B. Lin, B. Wang, and M. Zhang, "Research on lubrication in hot extrusion of G3 corrosion resistant Ni-based alloy tube II: calculation and application of glass lubricant viscosity-composition," *Acta Metallurgica Sinica*, vol. 47, pp. 374–379, 2011.

[13] L. X. Li, K. P. Rao, Y. Lou, and D. S. Peng, "A study on hot extrusion of Ti-6Al-4V using simulations and experiments," *International Journal of Mechanical Sciences*, vol. 44, no. 12, pp. 2415–2425, 2002.

[14] M. A. El-Bestawi, T. I. El-Wardany, D. Yan, and M. Tan, "Performance of whisker-reinforced ceramic tools in milling nickel-based superalloy," *CIRP Annals*, vol. 42, no. 1, pp. 99–102, 1993.

[15] A. Devillez, F. Schneider, S. Dominiak, D. Dudzinski, and D. Larrouquere, "Cutting forces and wear in dry machining of Inconel 718 with coated carbide tools," *Wear*, vol. 262, no. 7–8, pp. 931–942, 2007.

[16] E. Rabinowicz, L. A. Dunn, and P. G. Russell, "A study of abrasive wear under three-body conditions," *Wear*, vol. 4, no. 5, pp. 345–355, 1961.

[17] J. Zhou and J. Duszczyk, "Prevention of stick-stip tearing of a Duralcan AA6061-matrix composite during extrusion," *Journal of Materials Science Letters*, vol. 17, no. 19, pp. 1617–1619, 1998.

[18] P. G. Caceres, "Effect of microstructure on the abrasive wear properties of infiltrated tungsten alloys," *Materials Characterization*, vol. 49, no. 1, pp. 1–9, 2002.

[19] P. Matteis, G. Scavino, E. Quadrini, P. Perucci, and D. Firrao, "Damage of repeatedly nitrocarburised steel dies for aluminium extrusion," *Surface Engineering*, vol. 25, no. 7, pp. 507–516, 2009.

[20] Q. Fan, D. Zhou, L. Yang, J. Zhou, S. Yang, and Y. Yang, "Study on the oxidation resistance and tribological behavior of glass lubricants used in hot extrusion of commercial purity titanium," *Colloids and Surfaces A: Physicochemical and Engineering Aspects*, vol. 559, pp. 251–257, 2018.

[21] L. Lazzarotto, L. Dubar, A. Dubois, P. Ravassard, and J. Oudin, "Three selection criteria for the cold metal forming lubricating oils containing extreme pressure agents," *Journal of Materials Processing Technology*, vol. 80–81, pp. 245–250, 1998.

[22] V. Jayaseelan, K. Kalaichelvan, and S. V. ananth, "Lubrication effect on friction factor of AA6063 in forward extrusion process," *Procedia Engineering*, vol. 97, pp. 166–171, 2014.

[23] C. Huang, B. Zou, Y. Liu, S. Zhang, C. Huang, and S. Li, "Study on friction characterization and wear-resistance properties of Si_3N_4 ceramic sliding against different high-temperature alloys," *Ceramics International*, vol. 42, no. 15, pp. 17210–17221, 2016.

[24] D. Zhu, X. Zhang, and H. Ding, "Tool wear characteristics in machining of nickel-based superalloys," *International Journal of Machine Tools and Manufacture*, vol. 64, pp. 60–77, 2013.

[25] Y. Birol, "High temperature sliding wear behaviour of Inconel 617 and Stellite 6 alloys," *Wear*, vol. 269, no. 9–10, pp. 664–671, 2010.

[26] E. Broszeit, B. Matthes, W. Herr, and K. H. Kloos, "Tribological properties of r.f. sputtered Ti-B-N coatings under various pin-on-disc wear test conditions," *Surface and Coatings Technology*, vol. 58, no. 1, pp. 29–35, 1993.

[27] T. Murakami, S. Kajino, and S. Nakano, "High-temperature friction and wear properties of various sliding materials against aluminum alloy 5052," *Tribology International*, vol. 60, pp. 45–52, 2013.

[28] F. M. Wang, J. P. Xie, Y. Li, and A. Q. Wang, "Dry-sliding tribological characteristics of W80C20 composite under of magnetic field," *China Surface Engineering*, vol. 27, pp. 76–79, 2014.

[29] A. Skopp, M. Woydt, and K. H. Habig, "Tribological behavior of silicon nitride materials under unlubricated sliding between 22°C and 1000°C," *Wear*, vol. 181–183, pp. 571–580, 1995.

[30] F. H. Stott, "The role of oxidation in the wear of alloys," *Tribology International*, vol. 31, no. 1–3, pp. 61–71, 1998.

[31] P. Deng, C. Yao, K. Feng et al., "Enhanced wear resistance of laser cladded graphene nanoplatelets reinforced Inconel 625 superalloy composite coating," *Surface & Coatings Technology*, vol. 335, no. 5, pp. 78–86, 2017.